A Cytoplasmic Ca^{2+} Functional Assay for Identifying and Purifying Endogenous Cell Signaling Peptides in *Arabidopsis* Seedlings: Identification of AtRALF1 Peptide†

Miyoshi Haruta,† Gabriele Monshausen,‡ Simon Gilroy,‡ and Michael R. Sussman*,†

UW Biotechnology Center, University of Wisconsin, Madison, Wisconsin 53706, and Department of Botany, University of Wisconsin, Madison, Wisconsin 53706

Received January 25, 2008; Revised Manuscript Received April 18, 2008

ABSTRACT: Transient increases in the cytoplasmic Ca^{2+} concentration are key events that initiate many cellular signaling pathways in response to developmental and environmental cues in plants; however, only a few extracellular mediators regulating cytoplasmic Ca^{2+} singling are known to date. To identify endogenous cell signaling peptides regulating cytoplasmic Ca^{2+} signaling, *Arabidopsis* seedlings expressing aequorin were used for an in vivo luminescence assay for Ca^{2+} changes. These seedlings were challenged with fractions derived from plant extracts. Multiple heat-stable, protease-sensitive peaks of calcium elevating activity were observed after fractionation of these extracts by high-performance liquid chromatography. Tandem mass spectrometry identified the predominant active molecule isolated by a series of such chromatographic separations as a 49-amino acid polypeptide, AtRALF1 (the rapid alkalinization factor protein family). Within 40 s of treatment with nanomolar concentrations of the natural or synthetic version of the peptides, the cytoplasmic Ca^{2+} level increased and reached its maximum. Prior treatment with a Ca^{2+} chelator or inhibitor of IP_3-dependent signaling partially suppressed the AtRALF1-induced Ca^{2+} concentration increase, indicating the likely involvement of Ca^{2+} influx across the plasma membrane as well as release of Ca^{2+} from intracellular reserves. Ca^{2+} imaging using seedlings expressing the FRET-based Ca^{2+} sensor yellow cameleon (YC) 3.6 showed that AtRALF1 could induce an elevation in Ca^{2+} concentration in the surface cells of the root consistent with the very rapid effects of addition of AtRALF1 on Ca^{2+} levels as reported by aequorin. Our data support a model in which the RALF peptide mediates Ca^{2+}-dependent signaling events through a cell surface receptor, where it may play a role in eliciting events linked to stress responses or the modulation of growth.

Changes in the cytoplasmic Ca^{2+} concentration are thought to act as a second messenger for many growth, developmental, and environmental responses in plant cells. Ca^{2+} transporters on the plasma membrane and on intracellular membranes are known to be involved in these processes since genetically or pharmacologically disrupting such activities causes altered growth and altered responses to environmental stimuli (*1–5*). Depending on the type of signals, one or more transient elevations or "spikes" in Ca^{2+} concentration occur with their magnitude, frequency, duration, and spatial distribution believed to encode the nature of each signal (*6, 7*). Thus, Ca^{2+} oscillations and the consequent activation of Ca^{2+}-dependent signaling pathways are implicated in diverse physiological responses in plants (*8*). However, the mechanism(s) by which such Ca^{2+} changes are coupled to perception of extracellular signals remains mostly unidentified at the molecular level.

Cytoplasmic Ca^{2+} changes can be quantitatively measured in plants by injecting Ca^{2+} indicator dyes or expressing genetically encoded reporter proteins such as aequorin or cameleon in the cells of interest (*9–11*). Aequorin is a Ca^{2+}-dependent photoprotein isolated from the jellyfish *Aequoria* sp. The apoprotein can be expressed as a soluble protein in heterologous systems, such as *Arabidopsis*, and reconstituted in vivo to an active Ca^{2+}-dependent bioluminescent protein by incubation with its cofactor, coelenterazine. Upon reconstitution, the plant emits bioluminescence, with signal intensity reflecting Ca^{2+} levels. Indeed, such transgenic plants have been successfully used to measure Ca^{2+} increases in response to stimuli as varied as hormones, bacterial elicitors, abiotic stresses, gravistimuli, circadian rhythm, and blue light (*12–24*).

Measuring cytoplasmic Ca^{2+} is used in mammalian cells as a functional assay for the activation of cell surface receptors, such as G-protein-coupled receptor, ligand-gated ion channel (ionotropic receptor), and tyrosin kinase receptor (*25–28*). Binding of extracellular ligands such as peptide hormones and neurotransmitters to these receptors triggers concomitant cytoplasmic Ca^{2+} increases that relay signals to the downstream components of their pathways (*29*). By analogy to its action in mammals, glutamate is proposed to act as a key regulatory molecule based on its action causing cytoplasmic Ca^{2+} increases in *Arabidopsis* and the presence of ionotropic glutamate receptor-like genes in plant

* To whom correspondence should be addressed. Phone: (608) 262-8608. Fax: (608) 262-6748. E-mail: msussman@wisc.edu.
† UW Biotechnology Center.
‡ Department of Botany.

10.1021/bi8001488 CCC: $40.75
Published on Web 05/22/2008

genomes (*30, 31*). ATP was also suggested to be a potential extracellular signal in *Arabidopsis* based on observations of release of ATP into the appoplast upon stresses, ATP-induced cytoplasmic Ca^{2+} increases, and ATP regulation of gene expression (*32, 33*). However, despite such notable exceptions as glutamate and ATP, the number of endogenous regulators identified as generating plant Ca^{2+}-dependent signaling cascades remains small when compared to the number in mammalian systems.

Endogenous peptide hormones have recently emerged as important regulators for cell-to-cell communication in diverse plant signaling pathways such as defense response and cell proliferation (reviewed in ref *34*). These peptides are perceived by specific receptors located on the plasma membrane and, by analogy to animal peptide hormones, are expected to activate intracellular signal pathways involving secondary messengers such as the Ca^{2+} signaling cascade. In the *Arabidopsis* genome, there are more than 400 different receptor-like kinase genes with transmembrane domains (*35*). However, only a handful of ligands that biochemically interact with any of these cell surface receptors have been identified (*36–43*). These pairings of extracellular ligands and their cognate plasma membrane receptors are thought to be the tip of the iceberg, and there are likely to be many hundreds of additional molecules serving as ligands. To identify naturally occurring peptide ligands linked to plant Ca^{2+} signaling networks, we have developed an experimental strategy using an in vivo Ca^{2+} assay with aequorin-expressing *Arabidopsis* seedlings. The screen was based on the hypothesis that when extracted from the plant, these peptides would induce a cytoplasmic Ca^{2+} transient if added exogenously and that these Ca^{2+} increases could be detected using the aequorin reporter system.

We show here that the aequorin-expressing transgenic *Arabidopsis* seedling is an excellent tool for measuring changes in cytoplasmic Ca^{2+} at the whole plant level and amenable to screening utilizing a microplate format. Starting with *Arabidopsis* tissue extracts, we have used HPLC[1] and tandem mass spectrometry to fractionate, screen, purify, and identify the most predominant peptide active in this "Ca^{2+} elicitor" assay. Its sequence identifies it as AtRALF1 (At1g02900), a member of the RALF (rapid alkalinization factor) protein family. RALF was previously discovered in tobacco extracts, as a factor causing rapid alkalinization in the medium of suspension cells, and was proposed to be a new type of plant peptide hormone based on its ability to activate protein kinases and its inhibitory effect on root growth (*44*). RALF-induced cytoplasmic Ca^{2+} increase has not been previously reported. In our experiment, synthetic AtRALF1 peptide induced Ca^{2+} responses at nanomolar concentrations indistinguishable from that with endogenous AtRALF1. AtRALF1-induced Ca^{2+} elevation was further verified in the cells of the root using an independent assay of plants expressing the FRET-based Ca^{2+} sensor yellow cameleon (YC) 3.6 (*45*). Our results highlight the presence of endogenous hormone-like peptides in plant extracts that can be isolated for biochemical characterization. In addition, AtRALF1-induced cytoplasmic Ca^{2+} elevation found in this study provides new insight into intracellular signaling events that may link this peptide to the regulation of plant growth and development.

[1] Abbreviations: HPLC, high-performance liquid chromatography; RALF, rapid alkalinization factor; TFA, trifluoroacetic acid; SCX, strong cation exchange; MALDI-TOF, matrix-assisted laser desorption ionization time-of-flight; ACN, acetonitrile; GUS, β-glucuronidase; GFP, green fluorescent protein; FRET, fluorescent resonance energy transfer.

EXPERIMENTAL PROCEDURES

Cytoplasmic Ca^{2+} Assay in Arabidopsis Seedlings. To assay for changes in Ca^{2+} levels, an *Arabidopsis* line homozygous for a single insertion of a transgene encoding a cytoplasmically expressed apoaequorin driven by a cauliflower mosaic virus 35S promoter was used (*46*). Seeds were sterilized and plated on medium containing Murashige-Skoog salts (PhytoTechnology Laboratories, Shawnee Mission, KS), 3% (w/v) sucrose, and 0.4% (w/v) agar. The plates were kept at 4 °C for 2 days, exposed to red light (30 μmol m^{-2} s^{-1}) for 30 min, and incubated at 20 °C under continuous light (45 μmol m^{-2} s^{-1}) for 4 days. A single seedling was transferred into each well of a 96-well white microplate (Thermo Labsystems, Franklin, MA) containing 200 μL of liquid Murashige-Skoog medium supplemented with 2.5 μM coelenterazine cp (Sigma, St. Louis, MO) and incubated in the dark at 24 °C for 16 h. Into each well of the plate was added 45 μL of 20 mM potassium phosphate buffer (pH 7.5) containing a test substance or fractionated extract. The resulting luminescence emission was monitored using a microplate reader (SPECTRAFluor PLUS, Tecan Inc., Durham, NC) for 10 time points over approximately 160 s or 20 time points over 320 s. Calcium levels are presented as the sum of the luminescence counts that were obtained during the assay. All the data showing the cytoplasmic Ca^{2+} level as luminescent counts were collected using the assay described above. For dose−response analysis, GraphPad Prism (GraphPad Software, Inc., San Diego, CA) was used to fit a sigmoidal curve and calculate EC_{50}.

Plant Materials and Growth Conditions for Biochemical Assays. Approximately 250 seeds (*Arabidopsis thaliana*, Ws ecotype) were surface-sterilized and transferred to a 250 mL flask containing 75 mL of half-strength Murashige-Skoog salts and 1% (w/v) sucrose. Seedlings were grown under constant light (100 μmol m^{-2} s^{-1}) on an orbital shaker at 100 rpm (New Brunswick Scientific, Edison, NJ) at 24 °C. Two-week-old seedlings were harvested, frozen in liquid nitrogen, and stored at −80 °C until they were used.

Tissue Extraction and Separation for Screening. Tissue (200 g) was homogenized in 600 mL of 0.1% (v/v) TFA, filtered through Miracloth (Calbiochem, La Jolla, CA), and centrifuged at 10000*g* for 15 min at 4 °C. The supernatant was filtered through Whatman paper and applied onto a C4 reverse phase column (Vydac, 15 μm, 1 cm × 25 cm) equipped with a pump (HPLC Pump 501, Waters, Milford, MA). The captured material was eluted with 50% (v/v) ACN in 0.1% (v/v) TFA, dried down by a vacuum centrifuge, dissolved in 2 mL of 2% (v/v) ACN in 0.1% (v/v) TFA, and spun down. The supernatant was separated by being applied on a preparative C4 HPLC system with an isocratic run of 2% (v/v) ACN in 0.1% (v/v) TFA for 10 min and a gradient from 2 to 50% ACN in 0.1% TFA over 150 min (column, Vydac, 5 μm, 4.6 mm × 250 mm; HPLC, 2795 Separation Module, Waters) (Figure 1A). For enriching macromolecules in additional experiments (Figure 1B), the

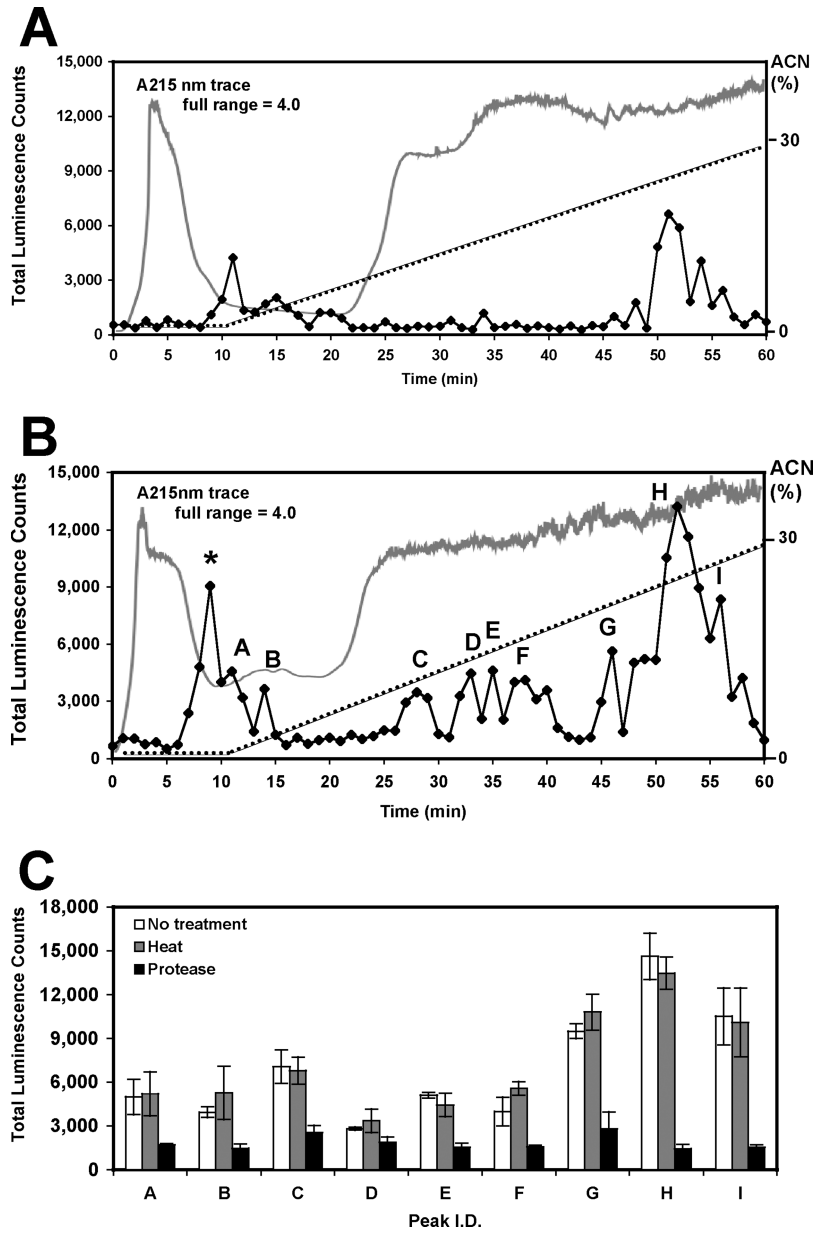

FIGURE 1: Multiple peaks of cytoplasmic Ca^{2+} increase activity are observed in HPLC-fractionated *Arabidopsis* seedling extracts. (A) Seedling extracts that were captured by a C4 preparative column were separated by C4 HPLC as described in Experimental Procedures. Forty-five microliters of each 500 μL fraction was dried, resuspended in 20 mM KH_2PO_4 buffer, and used for the aequorin Ca^{2+} assay. The UV (215 nm) trace is shown as a gray line. The dotted line indicates the ACN gradient. Relative Ca^{2+} increasing activity is expressed as the total luminescence counts and plotted with ◆ symbols and a black line. (B) Seedling extracts that were captured by a C4 preparative column and enriched in macromolecules by gel filtration were separated via C4 HPLC. Fractions were subjected to the Ca^{2+} assay as described for panel A. The peak denoted with an asterisk was due to the acidity of the fraction. Chromatograms shown in panels A and B are each one example of triplicate analyses. (C) The activity observed in peaks A−I of panel B was subjected to heat stability and protease sensitivity tests. Data are means ± the standard error of three samples, and the experiment was repeated twice with similar results.

material eluted in 50% (v/v) ACN from a C4 column was peptide-sized by being applied to a Sephadex G25 column (Sigma, 1.6 cm × 36 cm) that was equilibrated with 0.1% (v/v) TFA in water. The material recovered in the void volume was dried, dissolved in 2 mL of 2% (v/v) ACN in 0.1% (v/v) TFA, and separated by C4 HPLC as described above.

Protease Digestion and Heat Treatment of Active Fractions. Fractions (Figure 1C, A−H) determined to be active in eliciting a Ca^{2+} increase in the bioluminescence assay were dissolved in 20 mM potassium phosphate buffer (pH 7.5) and incubated with 0.1 mg/mL Pronase (Sigma) at 37 °C for 2 h. Heat treatment was carried out via incubation at 65 °C for 20 min.

Isolation of Peptide(s) Causing a Cytoplasmic Ca^{2+} Increase. Tissue (200 g) was homogenized in 600 mL of 0.1% (v/v) formic acid. The homogenate was filtered through Miracloth and centrifuged. The supernatant was filtered through Whatman paper and adjusted to 25% (v/v) ACN. The extract was applied onto a strong cation exchange (SCX) column that was equilibrated with 5 mM ammonium formate (pH 3.0) in 25% (v/v) ACN (flow rate of 5 mL/min, 12 μm, 7.5 mm × 75 mm, polySULFOETHYL A, The Nest Group, Southborough, MA). The active fraction was eluted with 1 M ammonium formate (pH 3.0) in 25% (v/v) ACN and concentrated. The resulting active fraction was loaded onto a Sephadex G25 column. The cytoplasmic Ca^{2+} increase activity eluting in the void volume was concentrated,

lyophilized, and separated on a C4 column (Vydac, 214TP54, 5 μm, 4.6 mm $\times$ 250 mm) at a flow rate of 0.5 mL/min with an isocratic run of 2% (v/v) ACN in 0.1% (v/v) TFA for 10 min and a gradient from 2 to 50% (v/v) ACN over 150 min. Chromatography was monitored at 215 nm (model 2996 photodiode array detector, Waters). The active fractions from the previous C4 column were purified on a SCX column (5 μm, 4.6 mm $\times$ 250 mm, polySULFOETHYL A) operating at a flow rate of 0.5 mL/min with an isocratic run of 300 mM ammonium formate (pH 3.0) in 25% (v/v) ACN for 10 min and a gradient run from 300 to 800 mM ammonium formate (pH 3.0) in 25% (v/v) ACN over 100 min. Chromatography was monitored by the fluorescent signal (excitation at 270 nm, emission at 310 nm, model 2475 fluorescence detector, Waters). The active fractions from the SCX column were fractionated with a C18 column (Vydac, 218TP54, 5 μm, 4.6 mm $\times$ 250 mm) with an isocratic run of 5% (v/v) ACN in 0.1% (v/v) TFA for 20 min and a gradient from 5 to 40% (v/v) ACN over 95 min. For Ca^{2+} assays, various volumes (10−200 μL) of chromatographic fractions were dried in a vacuum centrifuge and dissolved in 45 μL of 20 mM potassium phosphate (pH 7.5). Prior to the assay, the pH of test fractions was verified to be neutral using pH strips (EMD Biosciences, Inc., San Diego, CA).

Mass Spectrometry Analysis and Peptide Sequencing. Analytes were dissolved in 50% (v/v) ACN and 0.1% (v/v) TFA, mixed with the matrix, α-cyano-4-hydroxycinnamic acid (Aldrich) on a MALDI-TOF-MS plate (AnchorChip, Bruker), and air-dried. MALDI-TOF mass spectra were recorded using a Bruker (Billerica, MA) BIFLEX III instrument. For sequencing, 150 pmol of bioactive peptide was dissolved in 12 mM DTT in 100 mM ammonium bicarbonate, incubated at 50 °C for 40 min, modified with 6 mM iodoacetamide at 24 °C for 40 min, and purified by C18 HPLC as described above. The modified peptide was incubated with sequencing-grade modified trypsin at a trypsin:peptide ratio of 1:100 (w/w) (Promega, Madison, WI). Sequencing of trypsin-digested peptides was performed using tandem mass spectrometry (model 1100 series LC/MSD trap, Agilent Technologies, Palo Alto, CA). Peptides were separated using a C18 capillary HPLC system (3.5 μm, Zorbax SB300 C18, 75 μm $\times$ 150 mm) with a 20 to 50% (v/v) ACN gradient in 0.1% (v/v) formic acid over 80 min at a flow rate of 0.28 μL/min. Ion mass lists were searched using an in-house version of the MASCOT search tool (Matrix Science, London, U.K.) against an *Arabidopsis* protein database obtained from The Institute of Genomic Research (http://www.tigr.org/).

Peptide Synthesis, Modification, Purification, and Quantification. AtRALF1 peptide was synthesized at the 50 μmol scale at the Peptide Synthesis Facility, Biotechnology Center, University of Wisconsin. The synthetic peptide mixture (80 mg) was dissolved in 50 mL of 100 mM ammonium bicarbonate, stirred at 4 °C for 16 h, and lyophilized. Synthetic peptides were separated with a Sephadex G25 column and SCX and C18 HPLC as described above. The biologically active AtRALF1 peptide was detected by the aequorin Ca^{2+} assay and MALDI-TOF-MS. The concentration of isolated peptide was calculated using the method described by Pace et al. (*47*).

RNA Isolation and RT-PCR Analysis. Total RNA was extracted from various tissues of 4-week-old *Arabidopsis* plants using the RNeasy mini kit (Qiagen, Valencia, CA). The RNA template used for reverse transcription was first treated with DNase (Promega). Reverse transcription was carried out with SuperScript II reverse transcriptase as described by the manufacturer (Invitrogen, Carlsbad, CA). One microliter of each cDNA mixture was used as the template for PCR. The primer sequences for PCR are 5′-TGGACAAGTCCTTTACTCTGTTC-3′ and 5′-CCAAACA-ACTTCATGGATCA-3′ for AtRALF1 and 5′-CTGTTTC-CGTACCCTCAAGC-3′ and 5′-AGGGAAACGAAGACAGC-AAG-3′ for AtTUB4.

AtRALF1 Promoter Analysis. A 1185 bp DNA fragment of the AtRALF1 promoter region was PCR-amplified and cloned into pCAMBIA1301 (www.cambia.org). The resulting construct was introduced into plants via *Agrobacterium tumefaciens* GV3101. Plants were screened by hygromycin resistance and GUS immunoblotting. Four-day-old T2 seedlings were subjected to GUS staining at 37 °C for 6−16 h [50 mM sodium phosphate buffer (pH 7.2), 0.2% Triton X-100, 2 mM potassium ferrocyanide, 2 mM potassium ferricyanide, 15% methanol, and 2 mM 5-bromo-4-chloro-3-indolyl β-D-glucuronic acid]. Images were viewed with a Nikon E400 clinical microscope and recorded using a Spot Insight color digital camera (Diagnostic Instruments).

Imaging of Cytosolic Ca^{2+} Levels. To image cytosolic Ca^{2+} levels with cellular resolution, we used *Arabidopsis* expressing the FRET-based Ca^{2+} sensor yellow cameleon 3.6 (*44*). Four-day-old seedlings were transferred to purpose-built cuvettes and mounted in agarose containing $^1/_4$-strength Murashige-Skoog salts (pH ~ 6) supplemented with 1% (w/v) sucrose (modified from ref *48*). Shortly before an experiment, the agarose was dissected from around the root tip, and 100 μL of liquid medium containing $^1/_4$-strength Murashige-Skoog salts and 1% (w/v) sucrose (pH ~ 6) was added to the cuvette. For treatment with 100 nM AtRALF1, 100 μL of a 200 nM peptide solution (dissolved in $^1/_4$-strength Murashige-Skoog medium) was gently added to the cuvette. Roots were ratio imaged with a Zeiss LSM 510 laser scanning confocal microscope (Carl Zeiss Inc., Thornwood, NY) using a 40× water immersion, 1.2 numerical aperture, C-Apochromat objective. The YC3.6 Ca^{2+} sensor was excited with the 458 nm line of the argon laser and imaged using a 458 nm primary dichroic mirror and the Meta detector of the microscope. CFP and FRET-dependent Venus emission were collected at 473−505 and 526−536 nm, respectively. For time-lapse analysis, images were collected every 4 s. Bright-field images were acquired simultaneously using the transmission detector of the Zeiss LSM 510 microscope.

RESULTS

Optimizing Experimental Conditions of the in Vivo Cytoplasmic Ca^{2+} Assay. To identify endogenous plant peptides that could elicit Ca^{2+} signaling events, we used an *Arabidopsis* line expressing the Ca^{2+}-dependent luminescent protein aequorin as an assay tool to measure cytoplasmic Ca^{2+} changes after treatment with fractionated extracts from *Arabidopsis* seedlings. A single aequorin-expressing seedling and an aliquot of Murashige-Skoog medium containing the cofactor required to reconstitute active aequorin, coelenterazine cp, were dispensed into a well of a 96-well microtiter plate, and active aequorin was reconstituted in the plant

overnight. Subsequently, the intensity of luminescence emission from each seedling was recorded when each was treated with a fraction from seedling extracts. Prior to this screening, we first tested the effects of the various reagents used for extracting tissues and chromatographically separating biomolecules to assess whether these might yield artifactual increases in Ca^{2+}. The effect of adding Murashige-Skoog salts or phosphate buffer on the cytoplasmic Ca^{2+} level was negligible (Supporting Information, Table 1). The threshold concentration of NaCl causing cytoplasmic Ca^{2+} increases was determined to be in a range of 46−92 mM. Similar effects were observed when seedlings were treated with KCl. The Ca^{2+} increase in response to salts reached its maximum within 15 s of treatment and was comparable to the results reported in earlier studies of the cytoplasmic Ca^{2+} responses to salinity and osmotic stresses (*15*). Common reagents used in peptide and protein fractionations such as SDS, ACN, and TFA all caused cytoplasmic Ca^{2+} elevation when tested at the concentrations used during fractionation. On the basis of these results, compounds such as salts, organic solvents, and detergents were eliminated from the test solutions or kept at a much lower concentration than those shown to affect the Ca^{2+} assay.

Screening Arabidopsis Seedling Extracts for Ca^{2+} Increasing Activity. To screen for endogenous molecules inducing cytoplasmic Ca^{2+} increases, *Arabidopsis* seedlings were extracted and the extract was fractionated and then used for the aequorin-based seedling assay outlined above. Acidified water was used to initially extract tissues based on our assumption that it would denature most proteins whereas peptides are more stable in a low-pH environment. Peptides and other solutes from seedling extracts representing approximately 200 g of tissue were captured and concentrated with a preparative C4 column, fractionated with an analytical C4 HPLC column, and then used in the aequorin seedling Ca^{2+} assay (Figure 1A). A C4 column was chosen since it is a standard procedure for separating small proteins and polypeptides. In separate experiments, seedling extracts were applied to a preparative C4 column as described above, further enriched for peptide-sized (i.e., greater than 1000 Da) higher-molecular mass macromolecules by gel filtration chromatography, fractionated with an analytical C4 HPLC column, and then also subjected to the aequorin seedling Ca^{2+} assay (Figure 1B). The latter sample preparation method allowed us to eliminate the majority of inactive compounds and thus load more materials onto an analytical C4 HPLC column. The profiles of Ca^{2+}-eliciting fractions in the two sample preparation methods were similar and reproducible. Active peaks A−I observed in Figure 1B were further studied for their heat and protease sensitivity. Essentially, all the activity peaks were heat-stable and susceptible to protease treatment, suggesting that they are peptide-based molecules. To further characterize the compound(s) responsible, the peak with the greatest activity, peak H eluting at 52 min in Figure 1B, was subjected to additional biochemical tests. The activity in peak H was recovered from a SCX cartridge with salt concentrations of 500−1000 mM. Furthermore, in a dose−response experiment, a linear relationship was observed between its Ca^{2+} increasing activity and a dilution series from 1 to 1:1000 (data not shown).

Isolation and Structural Determination of AtRALF1, a Peptide Triggering a Cytoplasmic Ca^{2+} Increase. On the basis of the results of the biochemical characterization of activity peak H described above, we established an isolation procedure for the active factor(s) using the following series of sequential chromatographic steps: (1) SCX column, (2) gel filtration, (3) C4 reverse phase HPLC, (4) SCX HPLC, and (5) C18 reverse phase HPLC. In the first step of purification, the activity was captured with a SCX column, then eluted, and further size-separated by gel filtration (data not shown). The fractions containing Ca^{2+} mobilizing activity were enriched with an analytical C4 HPLC column (68−76 min in Figure 2A) and further purified using SCX HPLC (Figure 2B). The fraction exhibiting Ca^{2+} mobilizing activity that eluted at 76−77 min was subsequently isolated via C18 HPLC (Figure 2C), and the degree of its purity was determined with MALDI-TOF mass spectrometry (Figure 3A). Mass spectrometric analyses of the isolated fraction showed the presence of two peaks that were interpreted as the singly charged and doubly charged states of a molecule with a molecular mass of 5463 Da, which is consistent with the size of a peptide. Fragmenting this species ion using ESI ion trap MS/MS tandem mass spectrometry and searching the generated MS/MS peak lists by MASCOT software resulted in a match to At1g02900, a rapid alkalinization factor family protein similar to RALF precursor (*Nicotiana tabacum*), with a Mascot score of 39 and an *E* value of 0.031 (Figure 3B). The RALF peptide found here was termed AtRALF1 by following the nomenclature described by Olsen et al. (*49*). Considering that the mature form of RALF peptide has two pairs of disulfide bonds (*44*), the expected mass of the biologically active AtRALF1 peptide is 5463.09 Da. Thus, our observed peptide mass in the MALDI-MS analysis, 5463 Da, agrees with the theoretical mass of the AtRALF1 peptide. The biologically active peptide component capable of eliciting Ca^{2+} increases was found at amino acid positions 72−120 and so is likely processed from a 120-amino acid precursor polypeptide (Figure 3C). The yield of AtRALF1 peptide from 2.8 kg of ∼66000 two-week-old *Arabidopsis* seedlings was estimated to be 370 pmol on the basis of a comparison of the UV absorbance at 215 nm of the purified extract to that of chemically synthesized AtRALF1 peptide (see below).

Characterization of AtRALF1-Triggered Cytoplasmic Ca^{2+} Elevation. To test our hypothesis that the AtRALF1 peptide is indeed responsible for the Ca^{2+} mobilizing activity purified from our extracts, we examined the biological activity of a chemically synthesized peptide corresponding to the amino acid sequences located at residues 72−120 in AtRALF1 (Figure 3C). The synthetic peptide was first purified from a crude synthetic peptide mixture by standard HPLC fractionation. The synthetic peptide capable of mobilizing Ca^{2+} in the aequorin seedling assay was eluted at a retention time identical to that of the native peptide using C4, C18, and SCX HPLC (data not shown). A total of 35 nmol of biologically active synthetic peptide was recovered from 80 mg of the synthetic peptide mixture. The synthetic peptide triggered a luminescence (i.e., Ca^{2+}) signal of 15200 total counts at a concentration of 100 nM, while that of the native peptide isolated from *Arabidopsis* seedlings elicited 14726 counts at the same concentration. The time course of Ca^{2+} mobilization by the native and synthetic peptides was also very similar (Figure 4A).

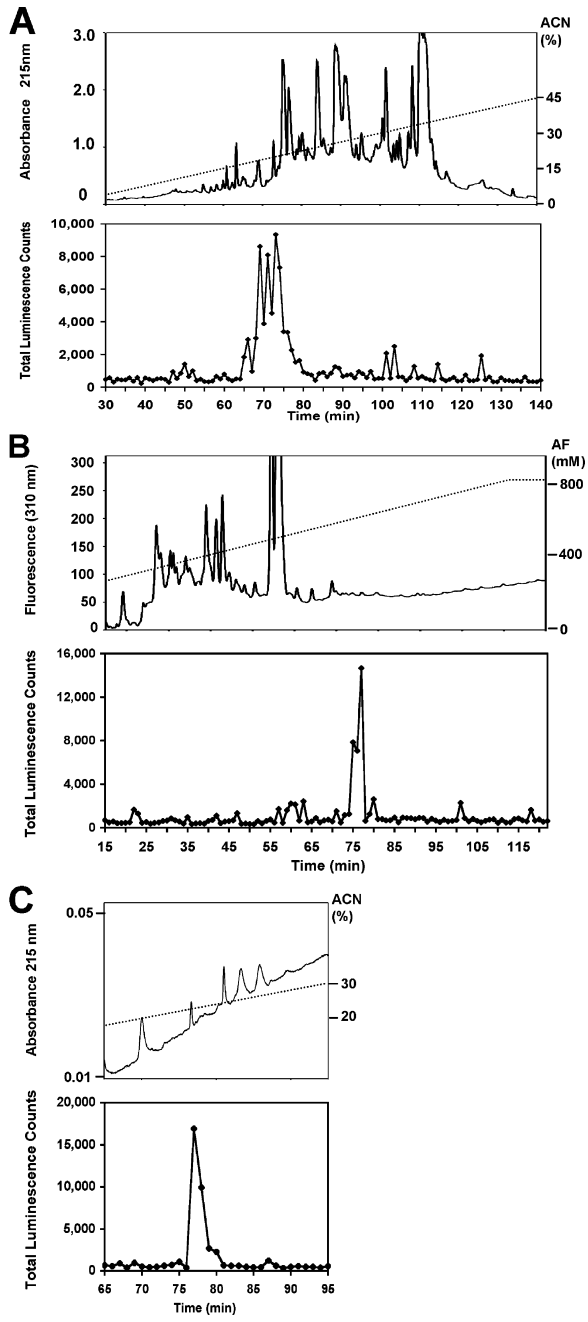

FIGURE 2: Ca^{2+} assay-guided purification of AtRALF1 from *Arabidopsis* seedling. (A) The absorbance (215 nm) of C4 HPLC fractions is shown with a black line (top panel). A liner gradient of ACN is shown with a dotted line. The Ca^{2+} mobilizing activity of the fractions from C4 HPLC is shown with ◆ symbols and a black line. (B) The fluorescence emission of SCX HPLC fractions is shown with a black line (top panel). A gradient of ammonium formate (AF) is shown with a dotted line. The Ca^{2+} mobilizing activity of the fractions from SCX HPLC is shown with ◆ symbols and a black line (bottom panel). (C) The absorbance (215 nm) of C18 HPLC fractions is shown with a black line (top panel). A gradient of ACN is shown with a dotted line. The Ca^{2+} mobilizing activity is shown with ◆ symbols and a black line. All chromatograms represent one example from multiple runs with similar results.

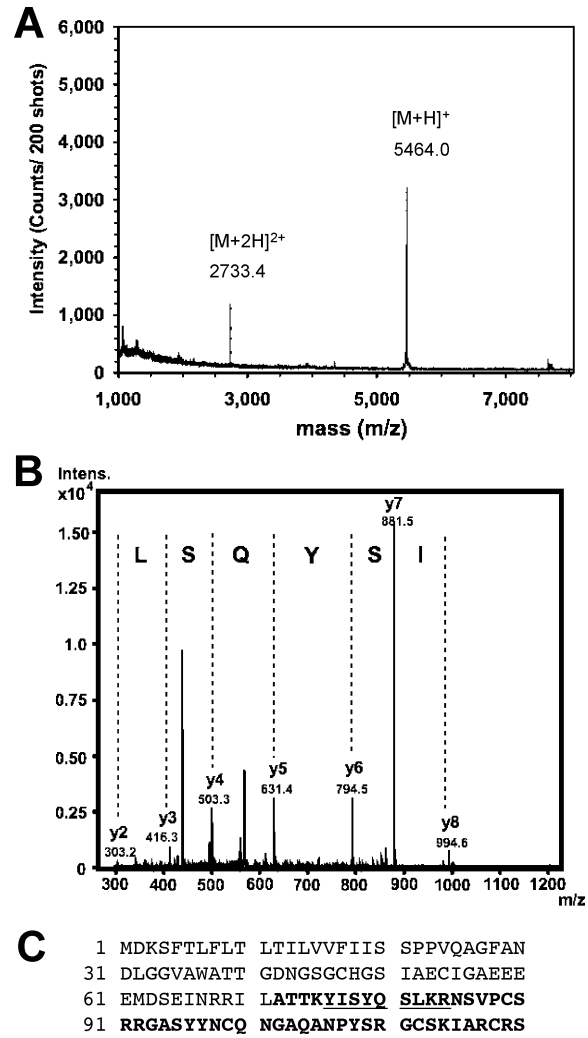

FIGURE 3: Mass spectrometric analyses and peptide sequence of AtRALF1. (A) MALDI-TOF-MS of the isolated biologically active molecule from peak H in Figure 1B. The peaks at *m/z* 5464 and 2733.4 correspond to singly charged and doubly charged states with a molecular mass of 5463 Da, respectively. (B) The tryptic peptide from the biologically active peptide was fragmented, and its amino acid sequence was obtained by ESI trap MS/MS. (C) The peptide sequence of AtRALF1 precursor protein was deduced from DNA sequence. The amino acid residues corresponding to the mature AtRALF1 polypeptide are shown with bold letters. The tryptic peptide fragment that was observed by MS and sequenced by MS/MS is underlined.

The dose−response relationship between AtRALF1 peptide and cytoplasmic Ca^{2+} increases was further characterized. AtRALF1 caused detectable increases in luminescence at <10 nM, and its apparent EC_{50} (the concentration inducing 50% of the maximum response) was 22 nM (Figure 4B). The AtARALF1-induced Ca^{2+} increase was saturated at 1 μM. At the end of the Ca^{2+} assay, for the highest concentration of AtRALF1 peptide tested, the remaining aequorin in the seedling was discharged using 1 M $CaCl_2$, confirming that the saturation of the AtRALF1-induced response was not due to the depletion of the available pool of aequorin. As a reference for the magnitude and efficiency with which AtRALF1 caused a Ca^{2+} increase, the effect of addition of exogenous ATP was characterized. ATP has been documented to cause a cytoplasmic Ca^{2+} increase and in our assay showed an apparent EC_{50} of 43 μM and saturation of the Ca^{2+} response at 1 mM, consistent with previously published observations [EC_{50} values of 2.6 μM determined by Demidchik et al. (*32*) and 50−750 μM by Jeter et al. (*33*)]. Since the Ca^{2+} concentrations in bathing media for these two studies and ours are comparable (~3 mM), the differences in the EC_{50} value for ATP are likely due to the differences in the level of aequorin expression or the types of coelentera-

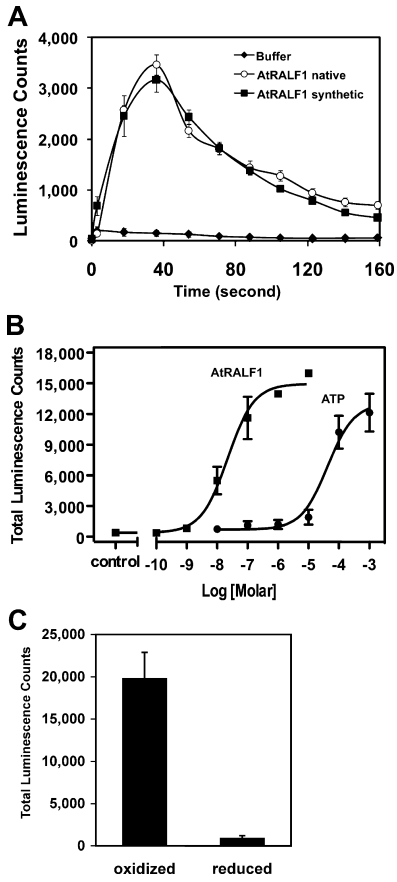

FIGURE 4: Characterization of AtRALF1-induced cytoplasmic Ca^{2+} elevation. (A) Kinetics of the Ca^{2+} increase triggered by 100 nM native and synthetic AtRAF1 peptide. The traces shown are the means of four measurements ± the standard error. (B) Dose−response effects of AtRALF1 (■) and ATP (●) on the cytoplasmic Ca^{2+} increase. (C) Cytoplasmic Ca^{2+} increase activity of the oxidized (i.e., properly refolded) and reduced (i.e., disrupted disulfide bonds) forms of AtRALF1 peptide.

zine used for the Ca^{2+} assay. While the maximum Ca^{2+}-dependent luminescence increases caused by AtRALF1 peptide and ATP are similar, the EC_{50} value for AtRALF1 was 1000 times lower than that for ATP.

The oxidized state of the four cysteine residues is known to be essential for the RALF-triggered extracellular alkalinization activity and root growth inhibition (*44*). To test whether the AtRALF1-induced Ca^{2+} increase activity was similarly sensitive to its oxidation state in our assay, peptides were reduced, modified, and subjected to the Ca^{2+} assay (Figure 4C). The loss of Ca^{2+} activity in the reduced form of AtRALF1 peptide is consistent with the loss of alkalinizing activity by modification of RALF peptide (*44*).

To examine whether the AtRALF1-induced cytoplasmic Ca^{2+} elevation arose from extracellular or intracellular sources, chemicals widely used to affect mobilization of Ca^{2+} from each of these sites were tested for their effect on the AtRALF1-induced Ca^{2+} elevation (Figure 5). Prior to the assay, seedlings were treated for 1 h with EGTA (Ca^{2+} chelator), LiCl (inhibitor of the phosphatidylinositol cycle), or neomycin (phosphatidylinositol interactor/PI specific phospholipase C inhibitor). Treating seedlings with those chemicals did not cause any visible changes in the seedlings. Prereatments with EGTA, LiCl, or neomycin inhibited AtRALF1-induced Ca^{2+} increases by 44, 40, and 26.3%, respectively.

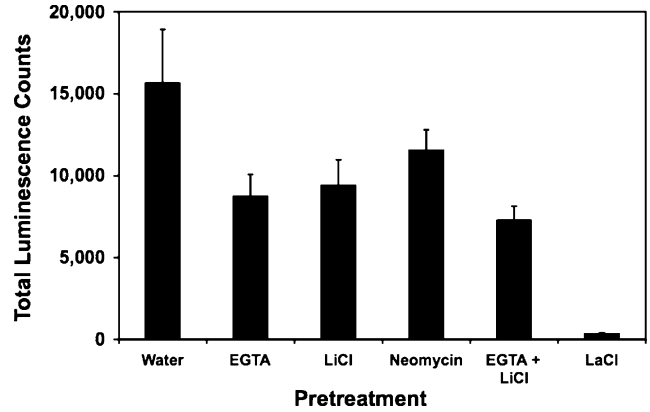

FIGURE 5: Suppression of AtRALF1-induced cytoplasmic Ca^{2+} increase by Ca^{2+} chelator and IP_3-signaling inhibitors. Seedlings were incubated with water, 20 mM EGTA, 20 mM LiCl, or 100 μM neomycin for 1 h prior to the Ca^{2+} assay. Results are means ± the standard error of four measurements and one representation of duplicated experiments.

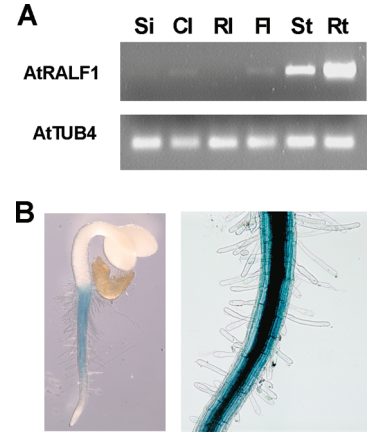

FIGURE 6: AtRALF1 expression analyses demonstrating the highest level of transcription in roots. (A) RT-PCR analyses of AtRALF1 and AtTUB4 expression in 4-week-old plants. Total RNA from silique (Si), cauline leaf (Cl), rosette leaf (Rl), flower (Fl), stem (St), and root (Rt) were subjected to RT-PCR. (B) AtARLF1 promoter activity visualized by GUS staining in germinating seedlings: whole seedling (left) and root hair zone (right).

Root Localization of AtRALF1 Gene Expression and Peptide Activities. To characterize the AtRALF1 gene at the molecular level, its expression in various tissues of adult *Arabidopsis* plants was surveyed by RT-PCR analyses. As shown in Figure 6A, the AtRALF1 transcript predominantly accumulated in root tissues. The GUS reporter assay was further used to identify cell types expressing the AtRALF1 gene. GUS staining was first detected in the root hair zone of seedlings with the highest intensity in the vascular bundles, cortex, and endodermis (Figure 6B). Staining in the hypocotyl and the veins of cotyledons was detected much later (data not shown). Similar AtRALF1 gene expression patterns were observed in the microarray analyses of the *Arabidopsis* root (*50*).

To identify organs and tissues exhibiting cytoplasmic Ca^{2+} elevation in response to treatment with AtRALF1 peptide, aequorin-based luminescence Ca^{2+} assays were carried out using dissected shoots and roots of 5-day-old seedlings. Noticeably, the largest Ca^{2+} mobilizing activity of AtRALF1 was mostly found in roots (Figure 7). Although this observation implies the root is more sensitive and responsive to AtRALF1, it is possible that the waxy cuticle covering aerial

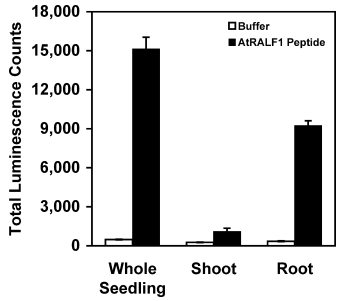

FIGURE 7: AtRALF1-induced cytoplasmic Ca^{2+} elevation in roots. Dissected shoots and roots of 5-day-old seedlings were incubated with coelenterazine for 16 h. The tissues were subjected to the aequorin Ca^{2+} assay for detection of AtRALF1-induced cytoplasmic Ca^{2+} responses. Data are means of four measurements with the standard error.

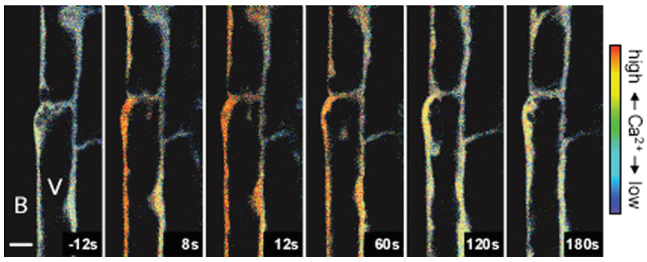

FIGURE 8: AtRALF1 triggers a rapid increase in cytoplasmic Ca^{2+} levels in root cells of *Arabidopsis*. Epidermal cells in the proximal elongation zone of the root were imaged every 4 s before and after treatment with AtRALF1 peptide. At time zero, 100 nM AtRALF1 peptide (at 2× concentration) was gently mixed into the medium. Numbers represent time. B denotes the bathing medium and V the vacuole.

tissues makes them less accessible for the exogenously applied peptides than roots, resulting in reduced Ca^{2+} responses. There was a consistent loss of luminescence signal in the sum of the dissected shoot and root compared to that in the whole seedling, which may be due to metabolic changes caused by dissecting (i.e., wounding), Ca^{2+} elevations during the handling needed for dissection dissipating some of the aequorin pool, or the requirement of tissue integration for the maximal AtRALF1-induced Ca^{2+} response.

To visualize the cellular dynamics of AtRALF1-induced cytoplasmic Ca^{2+} elevation, Ca^{2+} levels in the root were imaged using the GFP/FRET-based ratiometric Ca^{2+} sensor YC3.6. The roots of 4-day-old seedlings expressing the cameleon protein were treated with 100 nM AtRALF1 peptide, and the changes in cytoplasmic Ca^{2+} concentration were recorded (Figure 8). Cells in the epidermal cell of the proximal elongation zone showed clear Ca^{2+} increases upon treatment with AtRALF1 peptide. The cytoplasmic Ca^{2+} elevation was first detectable at the side facing the bathing medium, i.e., in contact with the medium containing the added AtRALF1. This increase then spread as a wave inward across the cell body to the side internal to the root. The time-lapse analyses of Ca^{2+} concentration changes indicated that AtRALF1-induced cytoplasmic Ca^{2+} elevation reaches its maximum within 60 s, agreeing with the kinetics of AtRALF1-induced Ca^{2+} elevation measured by the aequorin Ca^{2+} assay shown in Figure 4A. Adding the bathing medium alone did not change the FRET signal, i.e., did not elicit a detectable Ca^{2+} change (data not shown).

DISCUSSION

Although changes in the cytoplasmic Ca^{2+} concentration have been implicated in a broad range of signal pathways in plants (*8*), our understanding of how these changes relate to specific regulatory signaling pathways is incomplete. A wealth of data demonstrates peptides regulate animal physiology through second-messenger systems such as Ca^{2+} signaling cascades. In plants, there is a growing appreciation that endogenous peptide regulators may play a similarly critical role in plant growth and development. However, although peptides such as phytosulfokine are thought to regulate cell proliferation and CLAVATA3 regulates the balance between cell division and stem cell maintenance in the shoot meristem, both activities central to plant development, to date only in the case of the defense-related signal systemin has a peptide been shown to elicit changes in the classical second-messenger system, Ca^{2+} (*24, 34*). The changes in Ca^{2+} are thought to play key roles in triggering downstream responses elicited by systemin perception through the SR160 receptor-like kinase (RLK). The *Arabidopsis* genome contains approximately 400 RLKs with no identified ligand, suggesting there may be many peptide hormones operating via RLKs or other, as yet undefined, receptors still to be discovered in plants. We therefore screened the soluble peptide fraction from *Arabidopsis* for Ca^{2+} mobilizing activities as one strategy of identifying endogenous peptides with the potential to trigger Ca^{2+} signaling cascades within the plant. This approach identified AtRALF1, a 49-amino acid polypeptide, as a peptide hormone that triggers cytosolic Ca^{2+} increases consistent with receptor-mediated types of behavior. The previous discovery of RALF was based on its ability to alkalinize the medium of tobacco cell cultures (*44*). Our identification of AtRALF1 peptide as inducing cytoplasmic Ca^{2+} elevation illustrates an alternative means of searching for hormone-like peptides from plants. Furthermore, this study suggests the involvement of Ca^{2+}-related components in RALF-mediated intracellular signal transduction leading to root growth and development.

Our assay was based on the observation of which fractions from a soluble extract of *Arabidopsis* seedlings were capable of eliciting a Ca^{2+} increase in plants expressing the Ca^{2+}-dependent luminescent photoprotein aequorin. With the use of coelenterazine cp, an improved version of a cofactor for aequorin (*20, 26*), we were able to detect cytoplasmic Ca^{2+} increases in this single-seedling assay upon treatment with *Arabidopsis* tissue extract. Because whole-seedling measurements did not allow us to distinguish the (sub)population of cells in which Ca^{2+} increases occurred (*7, 51, 52*), it is not possible to correlate luminescence intensity with specific Ca^{2+} concentrations. Therefore, to semiquantitatively describe the treatment-induced changes in cytoplasmic Ca^{2+}, we summed the Ca^{2+}-dependent luminescence readouts obtained from a single seedling during the entire time course of treatment (160 or 320 s) and defined this sum as the total luminescence count elicited by the corresponding extract fraction. With the use of an aequorin-expressing line previously generated by Lewis et al. (*46*), we showed very small variation in luminescence emission among different seedlings (standard error between 6.6 and 26.9% of the mean). Demidchik et al. (*32*) noted that their cytoplasmic Ca^{2+} assay with an aequprin-expressing line displayed a standard error

averaging less than 15% of the means. Combined with the exceptionally high Ca^{2+} sensitivity of aequorin, these features enabled us to reproducibly identify fractions containing molecules with Ca^{2+} mobilizing activity (Figure 1A,B).

This screen identified nine fractions with Ca^{2+} mobilizing activity (Figure 1B,C, peaks A−I). Interestingly, the Ca^{2+} increases triggered by these fractions differed both in amplitude and in temporal pattern (Figure 1B, data not shown), indicating possible differences in the abundance of active molecules in each fraction, in the Ca^{2+} signatures of intrinsic signaling cascades, and/or in the location of target cells. The predominant activity isolated from fraction H, the fraction eliciting the strongest Ca^{2+} response, was identified as AtRALF1, a member of the rapid alkalinzation factor gene family (Figures 2 and 3). Both endogenous and synthetic AtRALF1 caused a cytoplasmic Ca^{2+} elevation that was rapid (Figures 4A and 8), saturable (Figure 4B), and specific (Figure 4C) as well as highly sensitive to the added peptide (Figure 4B). The EC_{50} for AtRALF1 obtained in our Ca^{2+} assay with whole seedlings was somewhat higher than EC_{50} values reported for the pH assay using tomato cell cultures [22 nM compared to 2 nM (Figure 4B) (*44*)]. This difference may indicate that tomato or tomato suspension cells have a higher sensitivity to RALF peptides than *Arabidopsis* seedlings. Alternatively, a lower EC_{50} value may be attributed to the greater density and accessibility of responsive cells in the homogeneous cell culture assay. If the response in the intact seedling is highly tissue specific, the increase in luminescence emanating from a small subset of cells may well be obscured against the background luminescence of unresponsive tissues, requiring higher peptide levels to trigger maximal detectable response, simulating lower sensitivity.

Indeed, our experiments suggest that it is the epidermis of the seedling root that shows the strongest cytoplasmic Ca^{2+} increase upon treatment with exogenous AtRALF1 (Figures 7 and 8). Ca^{2+} imaging using seedlings expressing the FRET-based Ca^{2+} sensor YC 3.6 revealed that AtRALF1 first triggered an elevation of Ca^{2+} at the side of an epidermal cell facing the external medium, which then quickly spread throughout the entire cell (Figure 8). This is consistent with the idea that RALF interacts with cell surface receptors, the identity of which is yet to be determined (*53*), and thus alters plasma membrane Ca^{2+} and H^+ transporter activities, resulting in a cytoplasmic Ca^{2+} increase and extracellular alkalinization (Figures 4, 7, and 8) (*44*). Similar scenarios seem to operate in early signaling events of pathogen-defense responses in plants where binding of the bacterial elicitor flagellin to a plasma membrane receptor is associated with rapid extracellular alkalinization and cytoplasmic Ca^{2+} elevation (*54*). The receptor-mediated Ca^{2+} transient induced by the *Phytophthora*-derived elicitor was also proposed to result primarily from an influx of Ca^{2+} from the extracellular space, though phospholipase C-dependent release of Ca^{2+} from intracellular stores also seems to contribute to the Ca^{2+} increase (*23*). In our study, we observed that the AtRALF-induced cytoplasmic Ca^{2+} increase was significantly reduced by the Ca^{2+} chelator EGTA and the IP_3 signaling inhibitor LiCl but was completely abolished by the Ca^{2+} channel blocker La^{3+} (Figure 5), consistent with both extra- and intracellular stores being involved in Ca^{2+} release.

Intriguingly, exogenous AtRALF1 elicited a strong elevation of cytoplasmic Ca^{2+} in the epidermis of the root tip, including meristem, elongation, and root hair zone (data not shown). However, both our analysis of *AtRALF1* gene expression using a promoter GUS assay and a previous root gene expression study using a microarray indicate that *AtRALF1* is expressed predominantly in the mature root with the highest expression levels occurring in the vascular tissues (Figure 6B) (*50*). This observation could imply that AtRALF1 peptide acts as a diffusible signal with a role in cell-to-cell communication. Alternatively, exogenously applied AtRALF1 may cross-react with a receptor for another member of the RALF family that consists of more than 34 isoforms in *Arabidopsis* (*49*), suggesting that specificity of RALF action would be imposed by a tight regulation of RALF localization. Given that AtRALF1 is constitutively expressed (Figure 6) (*50*) and translated into bioactive peptide (Figure 2) but seedlings can still respond to exogenously applied AtRALF1 peptide by a dose−response manner in the Ca^{2+} assay, it is likely that the availability of AtRALF1 peptide to target cells is the critical step activating or deactivating its downstream events.

The RALF peptide was discovered in tobacco extracts as a factor causing rapid alkalinization in the medium of suspension cells (*44*). A ubiquitous role for RALF peptides in plants was supported by the presence of functional orthologs in tomato, alfalfa, and poplar and the abundance of expressed sequence tags encoding RALF peptide(s) in 13 other plant species (*44, 55, 56*). Although RALF was first identified in a search for defense signals, it has since been shown to play a role in the regulation of root and root hair development. Exogenous RALF arrested root growth in *Arabidopsis* and tomato seedlings (*44*), while silencing RALF caused disruption of root hair development in *Nicotiana attenuata* (*57*). Consistent with such observations, the growth rate of *Arabidopsis* root hairs has been shown to correlate with oscillations in surface pH at the growing tip (*48*), with faster elongation during phases of lower pH and slower growth with periods of high wall pH. It is possible that AtRALF1 is a part of the mechanism regulating these pH oscillations, and silencing RALF has been demonstrated to cause altered surface pH oscillations in the root hair tip and disruption of root hair development in tobacco (*57*). In a growing root hair cell, cytoplasmic Ca^{2+} is elevated at the expanding tip with its levels likely regulated through the action of reactive oxygen species (ROS) generated by plasma membrane NADPH oxidase (*58*). In RALF-silenced tobacco, the root tip accumulated less ROS compared to the wild type, suggesting a model in which RALF is modulating the cytoplasmic Ca^{2+} level through a ROS-regulated plasma membrane Ca^{2+} transporter such as nonselective cation channel (*59*).

In summary, our results suggest the aequroin seedling assay system could be a powerful tool for isolating endogenous ligands related to Ca^{2+}-dependent signaling in plants. Our identification of AtRALF1 as a Ca^{2+} mobilizing ligand also provides insight into how members of this family of peptides may signal changes in plant growth and development. The observation that AtRALF1 can trigger Ca^{2+} changes in cells away from its major site of expression raises the intriguing possibility that the RALF family may represent a grouping of Ca^{2+} mobilizing peptides capable of utilizing the same receptor family to trigger Ca^{2+} signals, with specificity imposed by the spatial localization of each peptide.

Alternatively, AtRALF1 may act as a mobile signal coordinating growth between different tissues within the root. It will be necessary to trace the production, secretion, and translocation of AtRALF1 peptide to test this hypothesis. Further identifying AtRALF1 receptors and associating ion transporters will be a key next step in improving our understanding of the signal pathway for RALF-regulated root growth.

ACKNOWLEDGMENT

We thank Edgar Spalding for providing aequorin-expressing *Arabidopsis* seeds and helpful discussions, Sandra Austin-Phillips for the use of a microplate reader, Clark Nelson for luminescence data analyses, Gary Case for peptide synthesis, Heather Burch for plant materials, and Jim Brown and Amy Harms for technical advice and assistance with mass spectrometry and HPLC. Confocal imaging was performed at the UW-Madison Plant Imaging Center. This study was supported by research grants to M.R.S. from the U.S. Department of Energy and to M.R.S., S.G., and G.M. from the National Science Foundation.

SUPPORTING INFORMATION AVAILABLE

Effects of various reagents on cytoplasmic Ca^{2+} elevation examined by the aequorin Ca^{2+} assay. This material is available free of charge via the Internet at http://pubs.acs.org.

REFERENCES

1. Allen, G. J., Chu, S. P., Schumacher, K., Shimazaki, C. T., Vafeados, D., Kemper, A., Hawke, S. D., Tallman, G., Tsien, R. Y., Harper, J. F., Chory, J., and Schroeder, J. I. (2000) Alteration of stimulus-specific guard cell calcium oscillations and stomatal closing in *Arabidopsis det3* mutant. *Science 289*, 2338–2342.
2. Cheng, N. H., Pittman, J. K., Barkla, B. J., Shigaki, T., and Hirschi, K. D. (2003) The *Arabidopsis cax1* mutant exhibits impaired ion homeostasis, development, and hormonal responses and reveals interplay among vacuolar transports. *Plant Cell 15*, 347–364.
3. Peiter, E., Maathuis, F. J. M., Mills, L. N., Knight, H., Pelloux, J., Hetherington, A. M., and Sanders, D. (2005) The vacuolar Ca^{2+}-activated channel TPC1 regulates germination and stomatal movement. *Nature 434*, 404–408.
4. Schiøtt, M., Romanowsky, S. M., Bækgaard, L., Jakobsen, M. K., Palmgren, M. G., and Harper, J. F. (2004) A plant plasma membrane Ca^{2+} pump is required for normal pollen tube growth and fertilization. *Proc. Natl. Acad. Sci. U.S.A. 101*, 9502–9507.
5. Nakagawa, Y., Katagiri, T., Shinozaki, K., Qie, Z., Tatsumi, H., Furuichi, T., Kishigami, A., Sokabe, M., Kojima, I., Sato, S., Kato, T., Tabata, S., Iida, K., Terashima, A., Nakano, M., Ikeda, M., Yamanaka, Y., and Iida, H. (2007) *Arabidopsis* plasma membrane protein crucial for Ca^{2+} influx and touch sensing in roots. *Proc. Natl. Acad. Sci. U.S.A. 104*, 3639–3644.
6. Malhó, R., Moutinho, A., van der Luit, A., and Trewavas, A. J. (1998) Spatial characteristics of calcium signaling: The calcium wave as a basic unit in plant cell calcium signaling. *Philos. Trans. R. Soc. London, Ser. B 353*, 1463–1473.
7. Fasano, J. M., Massa, G. D., and Gilroy, S. (2002) Ionic signaling in plant responses to gravity and touch. *J. Plant Growth Regul. 21*, 71–88.
8. Sanders, D., Brownlee, C., and Harper, J. F. (1999) Communicating with calcium. *Plant Cell 11*, 691–706.
9. Tsien, R. Y. (1980) New calcium indicators and buffers with high selectivity against magnesium and protons: Design, synthesis, and properties of prototype structures. *Biochemistry 19*, 2396–2404.
10. Johnson, F. J., and Shimomura, O. (1972) Preparation and use of aequorin for rapid microdetermination of Ca^{2+} in biological systems. *Nat. New Biol. 237*, 287–288.
11. Miyawaki, A., Llopis, J., Heim, R., McCaffery, J. M., Adams, J. A., Ikura, M., and Tsien, R. Y. (1997) Fluorescent indicators for Ca^{2+} based on green fluorescent proteins and calmodulin. *Nature 388*, 882–887.
12. Schroeder, J. I., and Hagiwara, S. (1990) Repetitive increases in cytosolic Ca^{2+} of guard cells by abscisic acid activation of nonselective Ca^{2+} permeable channels. *Proc. Natl. Acad. Sci. U.S.A. 87*, 9305–9309.
13. Ehrhardt, D. W., Wais, R., and Long, S. R. (1996) Calcium spiking in plant root hairs responding to *Rhizobium* nodulation signals. *Cell 85*, 673–681.
14. Knight, H., Trewavas, A. J., and Knight, M. R. (1996) Cold calcium signaling in *Arabidopsis* involves two cellular pools and a change in calcium signature after acclimation. *Plant Cell 8*, 489–503.
15. Knight, H., Trewavas, A. J., and Knight, M. R. (1997) Calcium signaling in *Arabidopsis thaliana* responding to drought and salinity. *Plant J. 12*, 1067–1078.
16. Knight, M. R., Campbell, A. K., Smith, S. M., and Trewavas, A. J. (1991) Transgenic plant aequorin reports the effects of touch and cold-shock and elicitors on cytoplasmic calcium. *Nature 352*, 524–526.
17. Knight, M. R., Smith, S. M., and Trewavas, A. J. (1992) Wind-induced plant motion immediately increases cytosolic calcium. *Proc. Natl. Acad. Sci. U.S.A. 89*, 4967–4971.
18. Sedbrook, J. C., Kronebusch, P. J., Borisy, G. G., Trewavas, A. J., and Masson, P. H. (1996) Transgenic AEQUORIN reveals organ-specific cytosolic Ca^{2+} responses to anoxia in *Arabidopsis thaliana* seedlings. *Plant Physiol. 111*, 243–257.
19. Price, A. H., Taylor, A., Ripley, S. J., Griffiths, A., Trewavas, A. J., and Knight, M. R. (1994) Oxidative signals in tobacco increase cytoplasmic calcium. *Plant Cell 6*, 1301–1310.
20. Plieth, C., and Trewavas, A. J. (2002) Reorientation of seedlings in the earth's gravitational field induces cytosolic calcium transients. *Plant Physiol. 129*, 786–796.
21. Johnson, C. H., Knight, M. R., Kondo, K., Masson, P., Sedbrook, J., Haley, A., and Trewavas, A. (1995) Circadian oscillations of cytosolic and chloroplastic free calcium in plants. *Science 269*, 1863–1865.
22. Baum, G., Long, J. C., Jenkins, G. I., and Trewavas, A. J. (1999) Stimulation of the blue light phototropic receptor NPH1 causes a transient increase in cytosolic Ca^{2+}. *Proc. Natl. Acad. Sci. U.S.A. 96*, 13554–13559.
23. Blume, B., Nürnberger, T., Nass, N., and Scheel, D. (2000) Receptor-mediated increase in cytoplasmic free calcium required for activation of pathogen defense in parsley. *Plant Cell 12*, 1425–1440.
24. Moyen, C., Hammond-Kosack, K. E., Jones, J., Knight, M. R., and Johannes, E. (1998) Systemin triggers an increase of cytoplasmic calcium in tomato mesophyll cells: Ca^{2+} mobilization from intra- and extracellular compartments. *Plant Cell Environ. 21*, 1101–1111.
25. Stables, J., Green, A., Marshall, F., Fraser, N., Knight, E., Sautel, M., Milligan, G., Lee, M., and Rees, S. (1997) A bioluminescent assay for agonist activity at potentially any G-protein-coupled receptor. *Anal. Biochem. 252*, 115–126.
26. Dupriez, V. J., Maes, K., Le Poul, E., Burgeon, E., and Detheux, M. (2002) Aequorin-based functional assays for G-protein-coupled receptors, ion channels, and tyrosine kinase receptors. *Receptors Channels 8*, 319–330.
27. Saito, Y., Nothacker, H. P., Wang, Z., Lin, S. H. S., Leslie, F., and Civelli, O. (1999) Molecular characterization of the melanin-concentrating-hormone receptor. *Nature 400*, 265–269.
28. Wittamer, V., Franssen, J. D., Vulcano, M., Mirjolet, J. F., Le Poul, E., Migeotte, I., Brézillon, S., Tyldesley, R., Blanpain, C., Detheux, M., Mantovani, A., Sozzani, S., Vassart, G., Parmentier, M., and Communi, D. (2003) Specific recruitment of antigen-presenting cells by chemerin, a novel processed ligand from human inflammatory fluids. *J. Exp. Med. 198*, 977–985.
29. Berridge, M. J., Bootman, M. D., and Roderick, H. L. (2003) Calcium signaling: Dynamics, homeostasis and remodeling. *Nat. Rev. Mol. Cell Biol. 4*, 517–529.
30. Dennision, K. L., and Spalding, E. P. (2000) Glutamate-gated calcium fluxes in *Arabidopsis*. *Plant Physiol. 124*, 1511–1514.
31. Lam, H. M., Chiu, J., Hsieh, M. H., Meisel, L., Oliveira, I. C., Shin, M., and Coruzzi, G. (1998) Glutamate-receptor genes in plants. *Nature 396*, 125–126.
32. Demidchik, V., Nichols, C., Oliynyk, M., Dark, A., Glover, B. J., and Davies, J. M. (2003) Is ATP a signaling agent in plants? *Plant Physiol. 133*, 456–461.
33. Jeter, C. R., Tang, W., Henaff, E., Butterfield, T., and Roux, S. J. (2004) Evidence of a novel cell signaling role for extracellular adenosine triphosphates and diphosphates in *Arabidopsis*. *Plant Cell 16*, 2652–2664.

34. Matsubayashi, Y., and Sakagami, Y. (2006) Peptide hormones in plants. *Annu. Rev. Plant Biol. 57*, 649–674.
35. Shiu, S. H., and Bleecker, A. B. (2001) Receptor-like kinases from *Arabidopsis* form a monophyletic gene family related to animal receptor kinases. *Proc. Natl. Acad. Sci. U.S.A. 98*, 10763–10768.
36. Wang, Z. Y., Seto, H., Fujioka, S., Yoshida, S., and Chory, J. (2001) BRI1 is a critical component of a plasma-membrane receptor for plant steroids. *Nature 410*, 380–383.
37. Kachroo, A., Schopfer, C. R., Nasrallah, M. E., and Nasrallah, J. B. (2001) Allele-specific receptor-ligand interactions in *Brassica* self-incompatibility. *Science 293*, 1824–1826.
38. Matsubayashi, Y., Ogawa, M., Morita, A., and Sakagami, Y. (2002) An LRR receptor kinase involved in perception of a peptide plant hormone, phytosulfokine. *Science 296*, 1470–1472.
39. Scheer, J. M., and Ryan, C. A. (2002) The systemin receptor SR160 from *Lycopersicon peruvianum* is a member of the LRR receptor kinase family. *Proc. Natl. Acad. Sci. U.S.A. 99*, 9585–9590.
40. Chinchilla, D., Bauer, Z., Regenass, M., Boller, T., and Felix, G. (2006) The *Arabidopsis* receptor kinase FLS2 binds flg22 and determines the specificity of flagellin perception. *Plant Cell 18*, 465–476.
41. Yamaguchi, Y., Pearce, G., and Ryan, C. A. (2006) The cell surface leucine-rich repeat receptor for AtPep1, an endogenous peptide elicitor in *Arabidopsis*, is functional in transgenic tobacco cells. *Proc. Natl. Acad. Sci. U.S.A. 103*, 10104–10109.
42. Zipfel, C., Kunze, G., Chinchilla, D., Caniard, A., Jones, J. D., Boller, T., and Felix, G. (2006) Perception of the bacterial PAMP EF-Tu by the receptor EFR restricts *Agrobacterium*-meditated transformation. *Cell 125*, 749–760.
43. Jia, G., Liu, X., Owen, H. A., and Zhao, D. (2008) Signaling of cell fate determination by the TPD1 small protein and EMS1 receptor kinase. *Proc. Natl. Acad. Sci. U.S.A. 105*, 2220–2225.
44. Pearce, G., Moura, D. S., Stratmann, J., and Ryan, C. A. (2001) RALF, a 5-kDa ubiquitous polypeptide in plants, arrests root growth and development. *Proc. Natl. Acad. Sci. U.S.A. 98*, 12843–12847.
45. Nagai, T., Yamada, S., Tominaga, T., Ichikawa, M., and Miyawaki, A. (2004) Expanded dynamic range of fluorescent indicators for Ca^{2+} by circularly permutated yellow fluorescent proteins. *Proc. Natl. Acad. Sci. U.S.A. 101*, 10554–10559.
46. Lewis, B. D., Karlin-Neumann, G., Davis, R. W., and Spalding, E. P. (1997) Ca^{2+}-activated anion channels and membrane depolarizations induced by blue light and cold in *Arabidopsis* seedlings. *Plant Physiol. 114*, 1327–1334.
47. Pace, C. N., Vajdos, F., Fee, L., Grimsley, G., and Gray, T. (1995) How to measure and predict the molar absorption coefficient of a protein. *Protein Sci. 4*, 2411–2423.
48. Monshausen, G. B., Bibikova, T. N., Messerli, M. A., Shi, C., and Gilroy, S. (2007) Oscillations in extracellular pH and reactive oxygen species modulate tip growth of *Arabidopsis* root hairs. *Proc. Natl. Acad. Sci. U.S.A. 104*, 20996–21001.
49. Olsen, A. N., Mundy, J., and Skriver, K. (2002) Peptomics, identification of novel cationic *Arabidopsis* peptides with conserved sequence motifs. *In Silico Biology*, Vol. 2, 0039 (http://www.bioinfo.de/isb/2002020039/).
50. Birnbaum, K., Shasha, D. E., Wang, J. Y., Jung, J. W., Lambert, G. M., Galbraith, D. W., and Benfey, P. N. (2003) A gene expression map of the *Arabidopsis* root. *Science 302*, 1956–1960.
51. Dodd, A. N., Jakobsen, M. K., Baker, A. J., Telzerow, A., Hou, S., Laplaze, L., Barrot, L., Poethig, R. S., Haseloff, J., and Webb, A. A. R. (2006) Time of day modulates low-temperature Ca^{2+} signals in *Arabidopsis*. *Plant J. 48*, 962–973.
52. Kiegle, E., Moore, C. A., Haseloff, J., Tester, M. A., and Knight, M. R. (2000) Cell-type-specific calcium responses to drought, salt and cold in the *Arabidopsis* root. *Plant J. 23*, 267–278.
53. Scheer, J. M., Pearce, G., and Ryan, C. A. (2005) *Le*RALF, a plant peptide that regulates root growth and development, specifically binds to 25 and 120 kDa cell surface membrane proteins of *Lycopersicon peruvianum*. *Planta 221*, 667–674.
54. Gómez-Gómez, L., and Boller, T. (2002) Flagellin perception: A paradigm for innate immunity. *Trends Plant Sci. 7*, 251–256.
55. Haruta, M., and Constabel, C. P. (2003) Rapid alkalinization factors in poplar cell cultures. Peptide isolation, cDNA cloning, and differential expression in leaves and methyl jasmonate-treated cells. *Plant Physiol. 131*, 814–823.
56. Germain, H., Chevalier, E., Caron, S., and Matton, D. P. (2005) Characterization of five RALF-like genes from *Solanum chacoense* provides support for a developmental role in plants. *Planta 220*, 447–454.
57. Wu, J., Kurten, E. L., Monshausen, G., Hummel, G. M., Gilroy, S., and Baldwin, I. T. (2007) NaRALF, a peptide signal essential for the regulation of root hair tip apoplastic pH in *Nicotiana attenuata*, is required for root hair development and plant growth in native soils. *Plant J. 52*, 877–980.
58. Foreman, J., Demidchik, V., Bothwell, J. H. F., Mylona, P., Miedema, H., Torres, M. A., Linstead, P., Costa, S., Brownlee, C., Jones, J. D. G., Davies, J. M., and Dolan, L. (2003) Reactive oxygen species produced by NADPH oxidase regulate plant cell growth. *Nature 422*, 442–446.
59. Demidchik, V., and Maathuis, F. J. M. (2007) Physiological roles of nonselective cation channels in plants: From salts stress to signaling and development. *New Phytol. 175*, 387–404.

BI8001488